Lab sessions

- lab 1 : Solid State detector lab : Christian Gallrapp & colleagues (christian.gallrapp@cern.ch)
  meeting point , building 28 , second floor , room 15

- lab 2 : Resistive Plate Chambers : Roberto Guida (roberto.guida@cern.ch)
  meeting point : building 256

- lab 3 : Silicon Photo Multiplier : Dominik Dannheim & colleagues (dominik.dannheim@cern.ch)
  meeting point : building 21, first floor, room 067

Planning of a day

- 7:00 am bus leaves ESI for CERN
- 8:00 am CERN, building 33 (visitor center)
- 9:00 am starts of lab 1 (go directly to lab location see map)
- 12:30 end of lab 1
- lunch
- 13:30 start of lab 2
- 17:00 end of lab 2
- 17:30 bus leaves CERN for ESI

Groups

- group 1 : Aneliya , Julien, Maria, Zakariae
- group 2 : Tiina, Nicolas, Léonard, Aaron
- group 3 : Joakim, Olivier, Aurélie

Planning of labs

- First half-day (5/02) : group 1 : lab 1
  group 2 : lab 2
  group 3 : lab 3

- then circular permutation ...

	lab1 (SSD)	lab2 (RPC)	lab3 (SPM)
5/02 am	group 1	group 2	group 3
5/02 pm	group 3	group 1	group 2
12/02 am	group 2	group 3	group 1

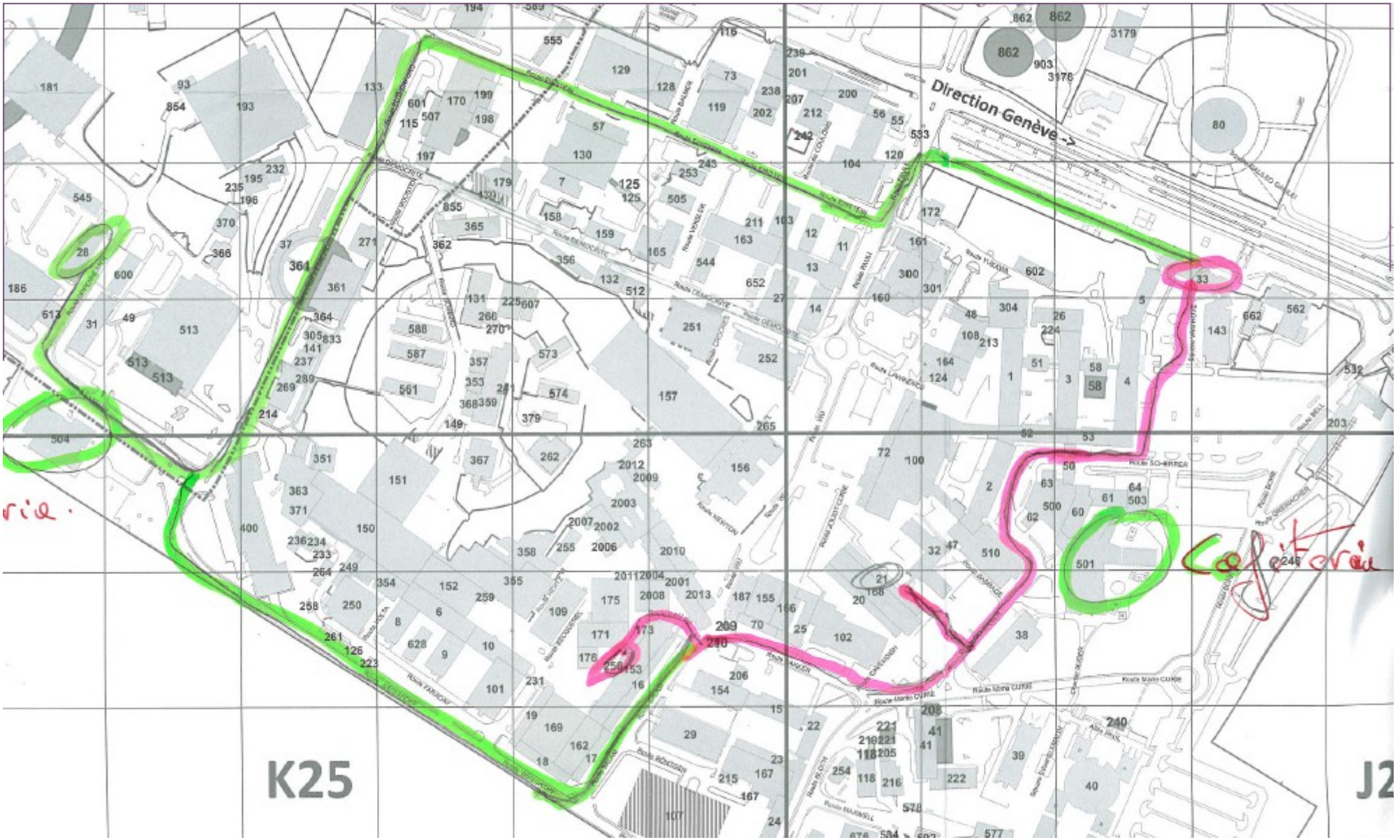
Direction Genève
K25
J2

Lab reports

- have to be finished before leaving school : should be sent to lab tutor (Christian lab 1, Roberto lab 2, Dominik Lab 3)
- 5-10 p max per lab evrything included
- introduction & general conclusion/summary
- plots with error bars , labels, units, captions ...
- concise style & good english
- writing for "experts" , skip details. Do not copy & paste.
- add all information needed in case the experiment should be redone
- test & verify your findings

ESIPAP School 2015 — SSD Lab-Session
Radiation Damage in Silicon Pad Sensors and LASER Characterization

5. + 12.02.2015

Introduction

The lab session illustrates the operation of silicon particle sensors as detector for ionising radiation. These sensors are based on a diode structure consisting of n- and p-doped silicon layers forming a pn-junction. The test structures basically consist of heavily p-/n-doped electrodes implanted in an intrinsic silicon bulk material.
For the operation of a silicon sensor an external reverse bias voltage is applied to form a space charge region. The bias voltage necessary to extend the space charge region over the full thickness of the device is the so-called full depletion voltage V_{dep}. With increasing bias voltage also the electric field within the depletion region increases.
The first part of the lab session (CV/IV measurement) demonstrates the development of the depletion region and the sensors capacitance as a function of the bias voltage. Further includes this part the determination and calculation of intrinsic sensor parameters relevant for the operation of the sensor such as the effective doping concentration and the electrical resistivity. The second part of the lab session (Transient Current Technique measurement) demonstrates how size and shape of the induced signal vary with bias voltage for front and back side illumination using a red LASER with a wavelength of 660 nm. Based on the measurement it becomes possible to calculate the mean velocity of the generated charge carriers.

Devices Under Test

The devices used in the lab session are simple pad sensors illustrated in Fig. 1. They are based on p-in-n diodes with a thickness of 300 µm and implants penetrating the material less than 2 µm.

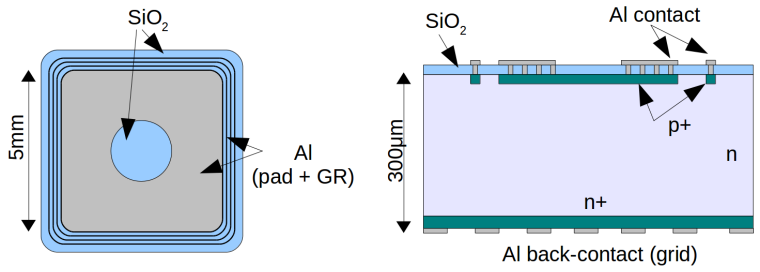

Figure 1: Layout of a p-in-n pad diode showing the top view (left) and the cross section (right). The pad structure includes the guard ring and the optical window on the top and the grid structure on the back.

The heavily p^+-doped ($1 \cdot 10^{18}$ atoms/cm^3) front implant forms the pn-junction with the n-doped

$(1 \cdot 10^{11}\,\text{atoms/cm}^3)$ bulk. The back side is also heavily n^+-doped $(1 \cdot 10^{18}\,\text{atoms/cm}^3)$ to build an ohmic contact. Front and back contacts are covered with a metal layer to build electrical connections for biasing and read-out. The front side contact comes with an optical window while the backside is covered with a grid to provide access for the illumination with a LASER. To reduce surface currents across the conductive sensor edge, the front pad is surrounded by one p^+ guard ring. If this guard ring is grounded it can be used to define the active area of the device to be $0.5 \cdot 0.5\,\text{cm}^2$.

Table 1: Devices under test and fluence.

CVIV	TCT	fluence
W331-D10	W331-C10	unirradiated
W331-D6	W331-Q4	$1 \cdot 10^{13}\,\text{p/cm}^2$
W331-P8	W331-Q3	$1 \cdot 10^{14}\,\text{p/cm}^2$

The samples which are studied during the lab session consist of 2 batches of 3 pad detectors fabricated by STMicroelectronics. These sample parameters are summarized in Tab. 1. While the samples for the CV/IV part are the bare pad sensors, the ones for the TCT part are already wire-bonded to PCBs. In order to investigate the radiation damage, four samples were irradiated with 24 GeV/c protons at the CERN Proton Synchrotron (PS). The corresponding fluence can also be found in Tab. 1.

1 Capacitance and Current Characterization

The CV/IV set-up is used to investigate the operational parameters of silicon sensors. It is based on the voltage dependent measurement of the capacitance and the leakage current of a device.

For the measurement a bias voltage is applied to the back side of the sample while the capacitance or leakage current are measured between the pad and the back electrode using a LCR meter or a picoamperemeter respectively. The cold chuck to mount the device under test and to control the temperature is depicted in Fig. 2 including the probe needles. A more detailed description is given by the supervisor, take appropriate notes if necessary. Starting from Poisson's equation given in Eq. 1 it is possible to calculate the electric field E and the electrostatic potential V inside an abrupt pn-junction, where N_{eff} is the effective doping density of the semiconductor.

$$\frac{dE}{dx} = \frac{d^2V}{dx^2} = -\frac{\rho}{\epsilon} = \frac{q}{\epsilon_{Si}\epsilon_0} N_{eff} \tag{1}$$

Solving Poisson's equation by integration gives the potential as a function of the depletion depth x as given in Eq. 2.

$$V(x) = \frac{q}{2\epsilon_{Si}\epsilon_0} |N_{eff}| x^2 \tag{2}$$

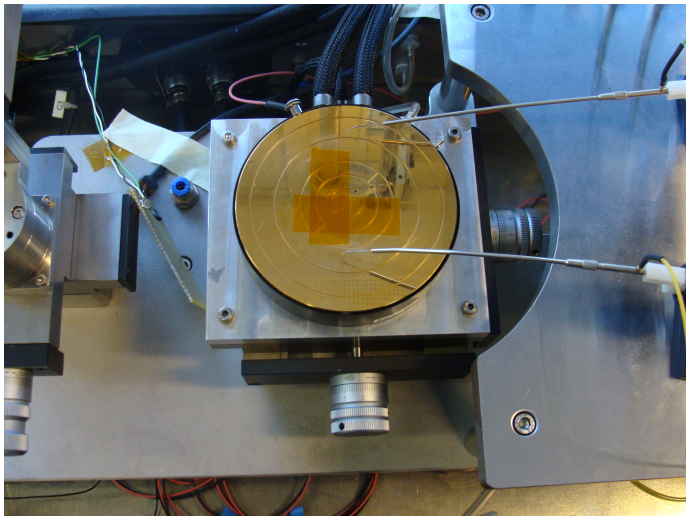

Figure 2: Cold chuck and probe needles of the CV/IV setup.

The depletion voltage V_{dep} of the diode is the voltage at which the depletion depth is equal to the thickness of the device (300 µm). The corresponding depletion width w given in Eq. 3 can be expressed as a function of the applied potential.

$$w(V_{dep}) = \sqrt{\frac{2\epsilon_{Si}\epsilon_0}{q|N_{eff}|}V_{dep}} \tag{3}$$

Above full depletion the sensor capacitance can be expressed as the capacitance of a plate capacitor given in Eq. 4 with a plate area A.

$$C(w) = \frac{\epsilon_{Si}\epsilon_0 A}{w} \tag{4}$$

The electrical resistivity ρ_{el} of the semiconductor given in Eq. 5 is defined as the inverse conductivity σ and given by the product of the effective doping concentration N_{eff} and the mobility μ of the majority carriers.

$$\rho_{el} = \frac{1}{\sigma} = \frac{1}{q\mu|N_{eff}|} \tag{5}$$

Table 2: Constants needed to calculate silicon properties

$\epsilon_{Si} = 11.9$	amu $= u = 1.660\,54 \cdot 10^{-27}$ kg (atomic mass unit)
$\epsilon_0 = 8.854 \cdot 10^{-14}\,A\,s\,V^{-1}\,cm^{-1}$	$\rho_{Si} = 2.33\,g/cm^3$
$q = 1.602 \cdot 10^{-19}\,C$	atomic weight/mass $= 28\,u$
$\mu_e = 1350\,cm^2\,V^{-1}\,s^{-1}$	$N_A = 6.022 \cdot 10^{23}\,mol^{-1}$ (Avogadro constant)
$\mu_h = 480\,cm^2\,V^{-1}\,s^{-1}$	

Aim of the CV/IV lab session

Observe the capacitance (CV) and current (IV) characteristics of silicon pad sensors before and after irradiation in function of the applied bias voltage. Investigate the key parameters of the sensor, i.e. depletion voltage, leakage current, effective doping concentration and electrical resistivity. Learn how these properties and the performance of silicon sensors change due to damage caused by ionizing and non-ionizing radiation.
Get familiar with the physical principles of semiconductors and pn-junctions. Discuss the definition of semiconductors and the working principle of a pn-junction.

Measurement procedure

- Check the connections for HV, pad and ground.
- Place the sample on the cold chuck and fix it with the vacuum. Use the microscope to position and connect the probe needles to the pad sensor and the guard ring using the corresponding screws on the probe holder.
- Remove the microscope and close the box.
- Check the polarity of the setup by applying ± 1V to your sensor.
- Set up the DAQ software (based on LabView) according to your needs - provide information about the voltage range, the maximum current and the temperature.
- For the CV measurement do the "open correction" to eliminate stray capacitance from the set-up instruments and cables.
- For the IV measurement choose "IV with two I-meter"

Tasks for the report

- Give a general description of the setup.
- Which polarity of bias voltage do you apply and why? How can you safely check this before?
- Plot $1/C^2$ and the leakage current in function of applied bias voltage for all measurements. (two plots)
- What are the variations between the different samples concerning the fluence? Discuss your observations in respect to the impact of radiation damage.
- Explain how you can extract the full depletion voltage V_{dep} and the end capacitance C_{end}.
- Extract the full depletion voltage V_{dep} and the end capacitance C_{end} from your measurements. Plot V_{dep} vs. fluence.
- Compare the leakage current at a fixed voltage (e.g. 300 V) for the different samples in one plot.

- How does the leakage current at 300 V change with fluence?
- Calculate the thickness d of the sample, the effective doping concentration N_{eff} of the bulk material and the ratio between phosphorus and silicon atoms.
- Comment on the sensitivity of your phosphorus concentration measurement.
- Determine the resistivity ρ_{el} of the bulk material.

2 Transient Current Technique (TCT)

Charge carriers generated by ionizing radiation within the active sensor region of a silicon particle detector get separated by the electric field and start to drift towards the electrodes. The movement of these charge carriers in the electric field introduces a current signal which is used to determine the path of a particle in a high energy physics experiment (tracking). In the case of a low electric field strength, the drift velocity v of the charge carriers is proportional to the local electric field strength E and the mobility μ of the charge carrier.

$$v = \mu \cdot E \tag{6}$$

As the induced signal is related to the electric field configuration in the sensor it became necessary to develop means to determine the exact shape of the electric field. Especially for the characterization of particle detector properties after irradiation these measurement techniques provide the possibility to understand the formation of the field. Furthermore, this information makes it possible to modify the sensor layout to increase charge collection properties after irradiation and to improve the sensor performance. One of these techniques is the Transient Current Technique (TCT) which injects e/h-pairs by irradiating the sensor surface with a monochromatic LASER.

The movement of the generated charge carriers induces a current signal i_{ind} which is defined by the Ramo theorem given in Eq. 7. This signal can be used to study the electric field profile within a sensor.

$$i_{ind} = -n \cdot q \cdot v \cdot E_v \tag{7}$$

Here, the induced signal i_{ind} corresponds to the number of charge carriers n with the charge q and the instantaneous velocity v moving in the weighting field E_v [1].
To add a spatial component of the measurement a focused LASER with a beam spot diameter of few micro meters provides the means to scan over the detector surface. The localized charge clouds generated within the active detector region start to drift instantaneously due to the force of the electric field. In the case of sensors with parallel plate geometries such as the diodes in Tab. 1 corresponds the weighting field to $E_v = 1/d$. Presuming a low electric field strength ($< 10\,V\mu m^{-1}$) and replacing the weighting field makes it possible to combine Eq. 6 and Eq. 7 to see the correlation

between the induced current and the electric field within the sensor.

$$i_{ind} = \frac{nq\mu E}{d} \tag{8}$$

As the induced current is directly linked to the number of injected photons is the signal shape more important than the exact value of the current. The evolution of the induced current with the drift time on the other hand makes it possible to extract the mean drift velocity and the field profile. This becomes possible by imposing boundary conditions over the drift time and the total voltage drop on the detector. This non trivial analysis becomes more difficult for irradiated samples when charge trapping takes place in the detector.

(a) front illumination

(b) back illumination

Figure 3: TCT measurement illustrating the two illumination methods and the corresponding charge movement in the sensor bulk.

Depending on the illumination direction can either the movement of holes or electrons be investigated. Both measurement configurations are illustrated in Fig. 3. As the absorption length of this wavelength in silicon is in the order of 3 µm are the e/h-pairs generated close to the surface of the sensor. Depending on the illumination direction one of the charge carries starts to drift towards the electrode at the opposite side of the diode while the others are immediately collected. As the induced signal is related to the movement of the charge carriers are only the moving charges contributing to the measured signal.
Due to the inhomogeneity of the electric field within the silicon diode is the induced current in Eq. 8 not constant but varies while the charge cloud drifts through the material. This behaviour is illustrated in Fig. 4 showing LASER induced signal pulses for for electron and hole movement in the a diode. Due to the different drift velocity of electrons and holes varies the signal width shown in Fig. 4.

Aim of the TCT lab session

Get a general understanding of the Transient Current Technique and learn how to extract sensor properties from the measurements.
In a first step you will discuss the TCT setup and get an introduction to the different components and the readout circuit. This discussion will also focus on the development of the electric field in the diode and its impact on the performance of the sensor and the measurement.

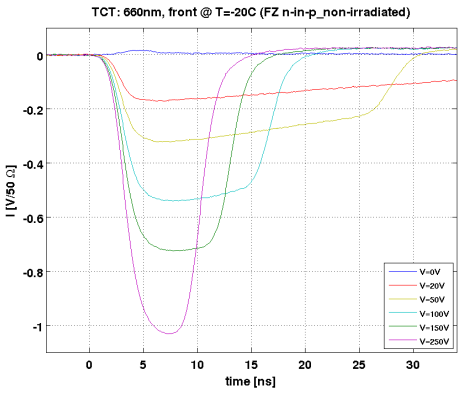

(a) front signal

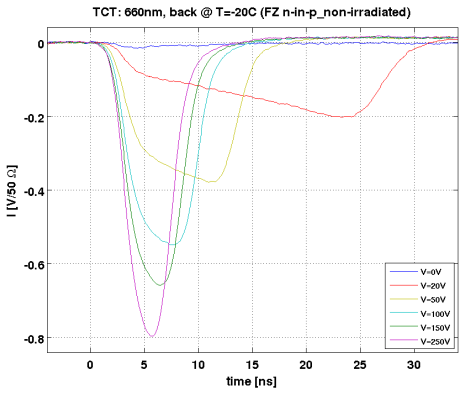

(b) back signal

Figure 4: Induced current signal for holes and electrons in Fig. 4(a) and Fig. 4(b) respectively. Remarkable is the variation of the signal width and shape for the different charge carriers.

In order to determine the sensor properties in function of the applied bias voltage and fluence the diodes given in Tab. 1 need to be measured with the TCT setup. During this step you will perform for each diode measurements for different bias voltages and from both sides. The measured signal will be directly compared and discussed. Finally you will use the obtained data to extract the mean velocity and mean mobility of the different charge carries.

Measurement procedure

- Check that all power supplies are ramped down to 0 V before modifying the setup.
- Mount the PCB with the sensor in the setup and connect the readout and the temperature control.
- Check that the readout circuit inside the shielded box is correctly set up.
- Close the shielded box.
- Ramp the different bias voltages up.
- Switch on the LASER.
- Save the measurement shown in the scope for three different voltages.
- Change the illumination direction
- Save the measurement shown in the scope for three different voltages.
- Turn off the LASER and ramp down the bias voltage before you swap the samples

Tasks for the report

- Give a general description of the setup.

- What is the purpose of the amplifier?
- Discuss the bias tee circuit.
- Plot for each sample the measured signals for electrons and holes individually. (six plots)
- Discuss the signal shape of the measurements. Focus on the differences between electron and hole movement.
- Explain how to calculate the mean velocity of charge carriers
- Calculate the mean velocity for electrons an holes. Plot your results in function of the applied bias voltage. Also summarize your results in a table.
- Calculate the mobility and summarize it in a table. Compare the results with the mobility given in Sec. 1.

References

[1] S. Ramo, *Currents Induced by Electron Motion*, Proceedings of the IRE, vol. 27, p. 584, 1939.

Contacts

CERN SSD - Solid State Detector Lab:

Marcos Fernandez Garcia	marcos.fernandez@cern.ch
Christian Gallrapp	christian.gallrapp@cern.ch
Michael Moll	michael.moll@cern.ch
Hannes Neugebauer	hannes.neugebauer@cern.ch

The Resistive Plate Chamber detectors at the Large Hadron Collider experiments

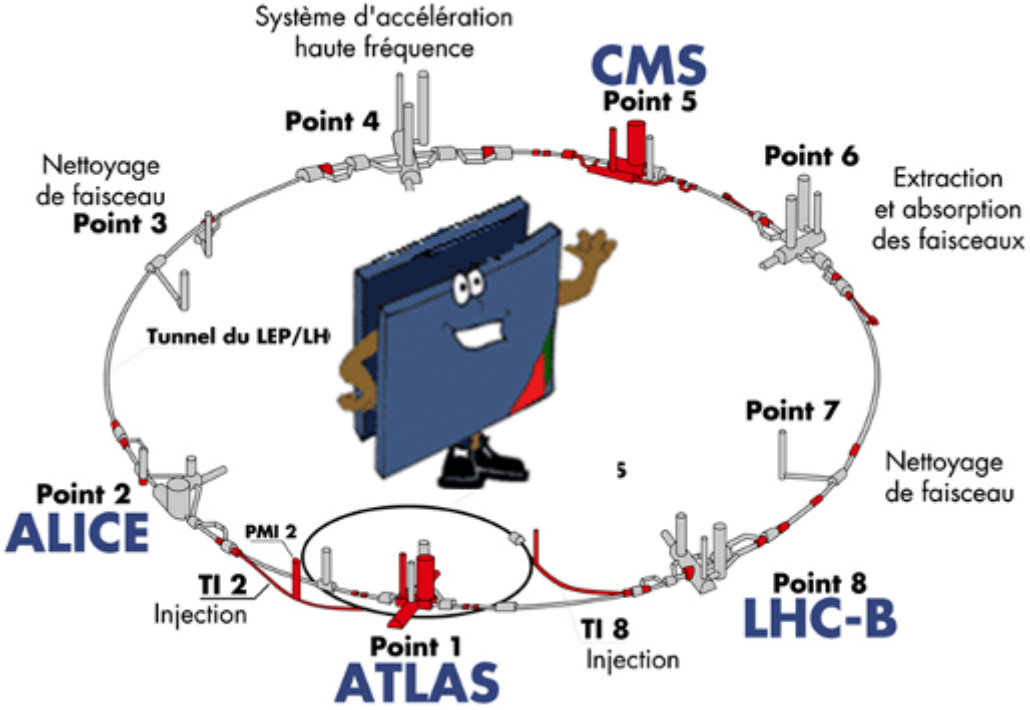

Ionization chambers

Ionizing particles are producing primary ionization (free electrons and ions)
Few primary electrons can gain enough energy to produce further ionization

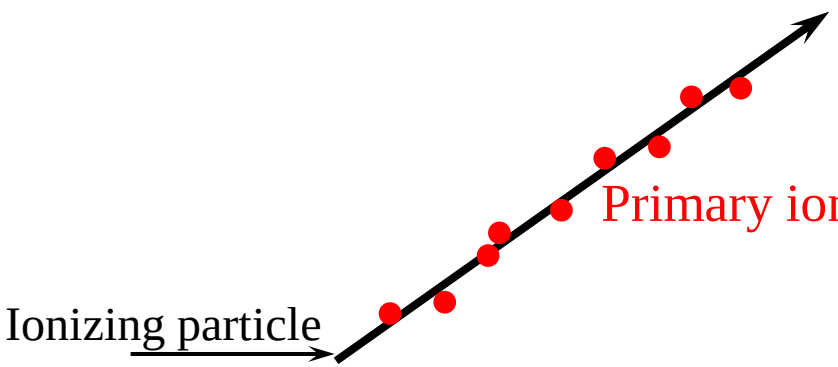

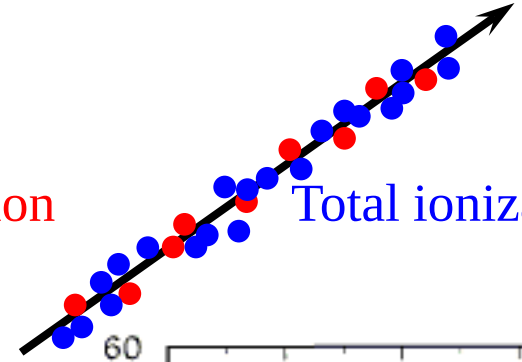

n_{total}: total number e^-/Ion

ΔE: total energy loss

W_i: <energy loss>/(total number e^-/Ion)

$$n_{total} = \frac{\Delta E}{W_i} = \frac{\frac{dE}{dx}\Delta x}{W_i}$$

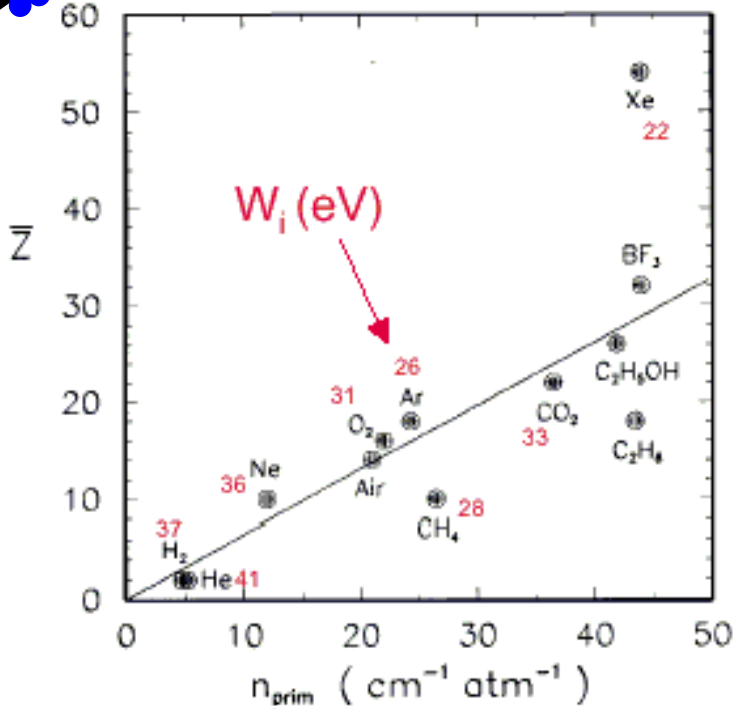

Ionization chambers

Primary ions/electrons start drifting under the effect of the applied electric field

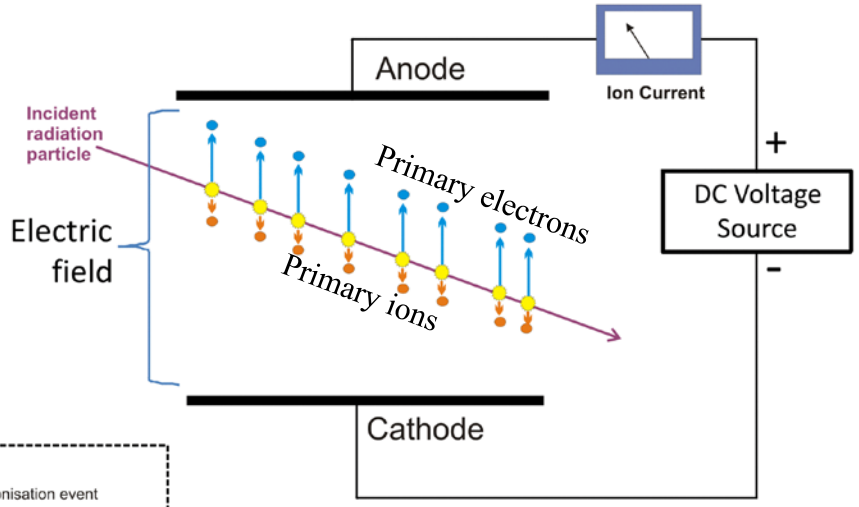

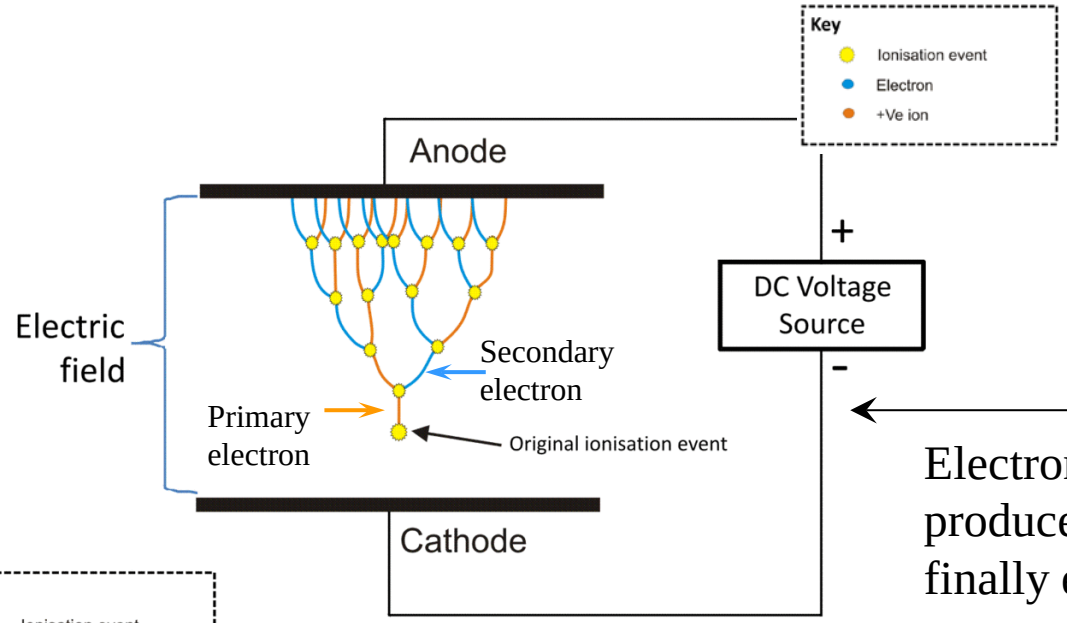

Electrons can gain enough energy to produce secondary ionization and finally electron avalanche

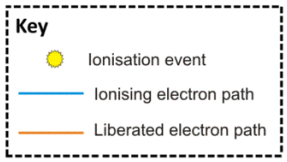

Not to sca

Ionization chambers

The ionization process depends strongly on the gas type

- Air is not a good medium ☹
- Right mixture can be quite complex and difficult to find

Typical gas mixture components:

- Bulk gas: Argon – common, not toxic, …
- quenching gas added for stability (photons absorption): CO_2, CH_4, iC_4H_{10}, …
- Others: CF_4, SF_6, …

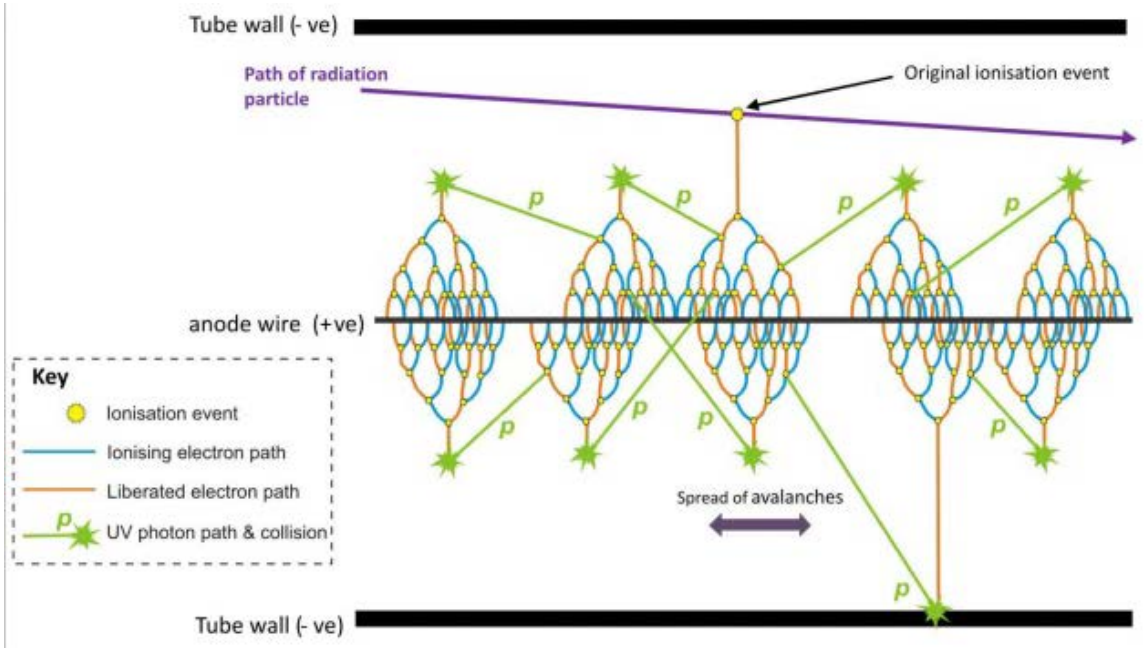

Process is affected even by presence of very low concentration of impurities

Ionization chambers

- Several applications
- Different geometries, gas mixtures, combination of effects, …

- drift tube

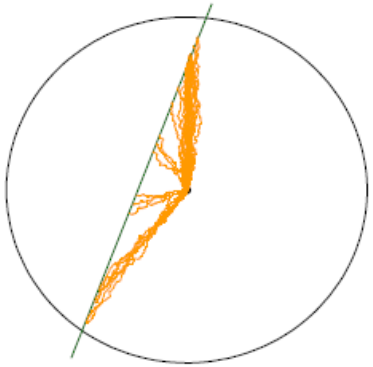

- RPC

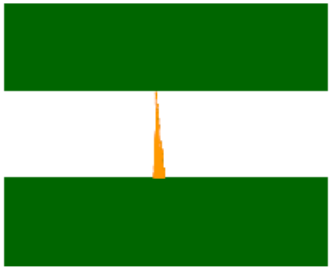

- GEM

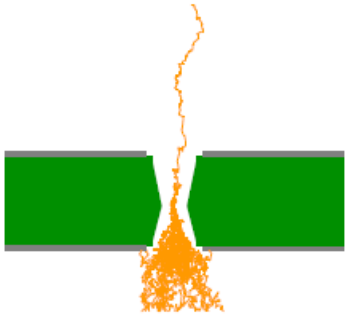

- Micromegas/InGrid

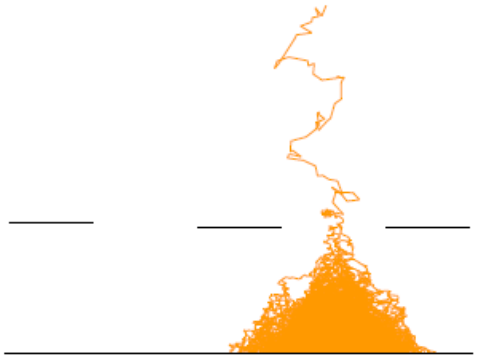

RPC from prototypes to large systems

1949: Keuffel → first Parallel Plate Chamber

1955: Conversi used the "PPC idea" in the construction of the flash chambers

1980: Pestov → Planar Spark chambers – one electrode is resistive – the discharge is localised

1981: Santonico → development of Resistive Plate Chamber – both electrode are resistive

RPC applications:

'85: Nadir (n-n\bar oscillation) – 120 m^2 (Triga Mark II – Pavia)
'90: Fenice (J/Ψ → n-n\bar) – 300 m^2 (Adone – Frascati)
'90: WA92 – 72 m^2 (CERN SPS)
'90: E771– 60 m^2; E831 – 60 m^2 (Fermilab)

1992: development of RPC for high particle rate → towards application at LHC

1994-1996: L3 – 300 m^2 (CERN-LEP)
1996-2002: BaBar – 2000 m^2 (SLAC)

Identikit of RPC detectors for LHC

Basic parameter for a detector design:

- Gap width
- Single gap/double gap/multi gap design
- Gas mixture
- Gas flow distribution
- Bakelite bulk resistivity
- Linseed oil electrode coating

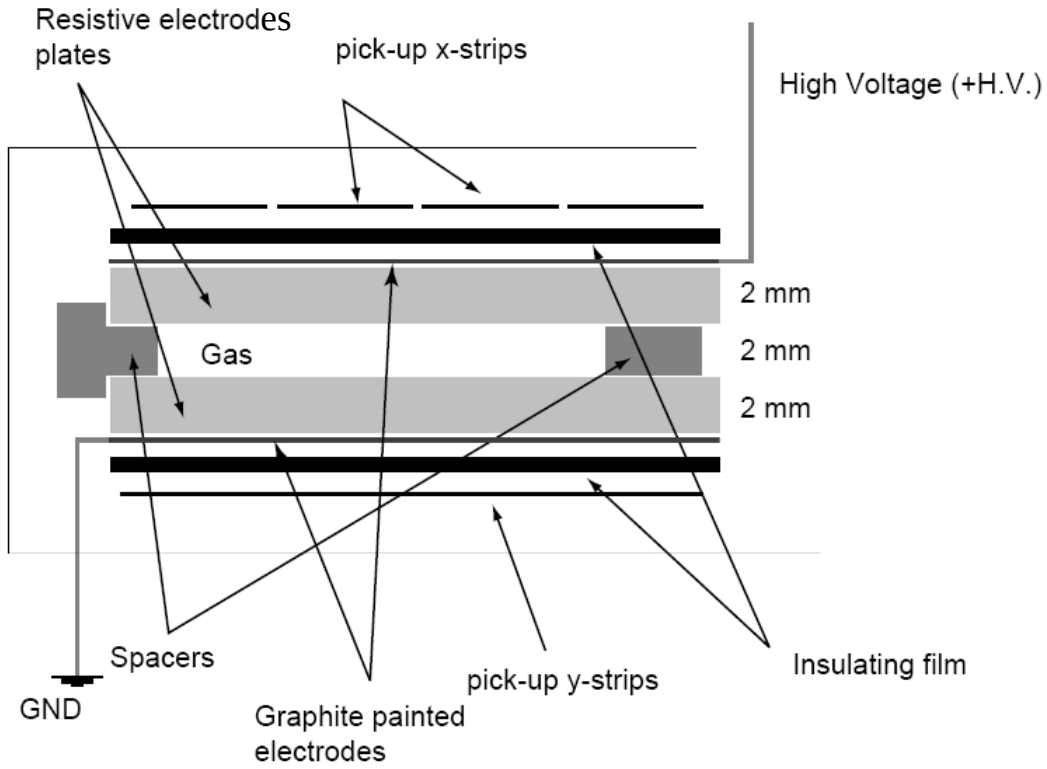

Why RPC?

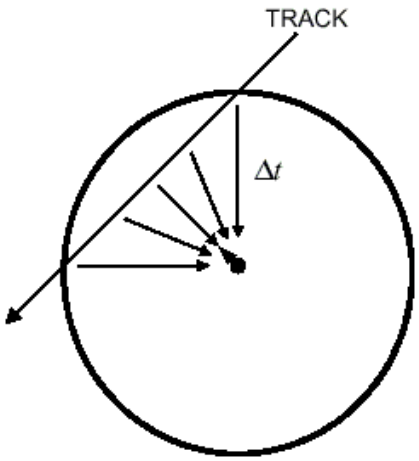

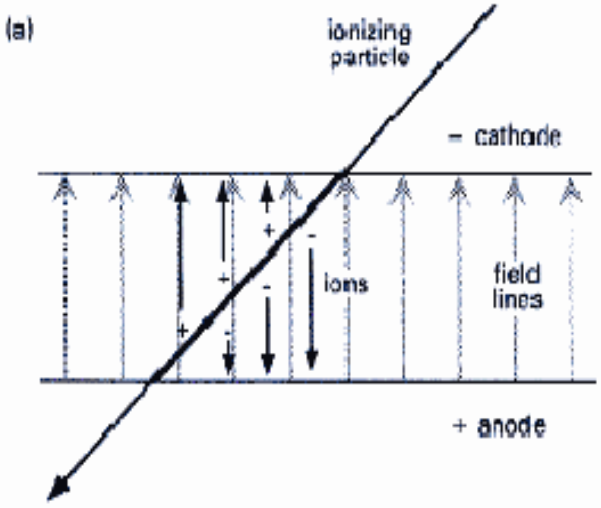

Drift chambers (cylindrical geometry) have an important limitation:
Primary electrons have to drift close to the wire before the charge multiplication starts
→limit in the time resolution ~ 0.1μs
→Not suitable for trigger at LHC

+ In a parallel plate geometry the charge multiplication starts immediately (all the gas volume is active).
+ much better time resolution (~ 1 ns)
+ less expensive (~ 100 €/m^2)

However:

-Smaller active volume
-Electrical discharge may start more easily
-Relatively expensive gas mixture
-Quite sensitive to environmental conditions (T and RH)

RPCs for LHC experiments

Where are the RPCs systems at LHC?

ATLAS experiment:

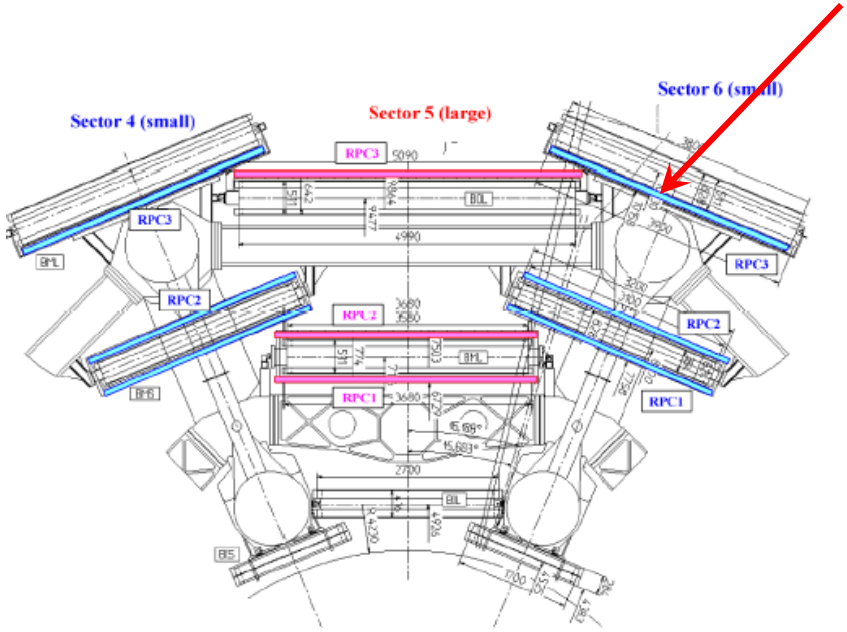

CMS experiment:

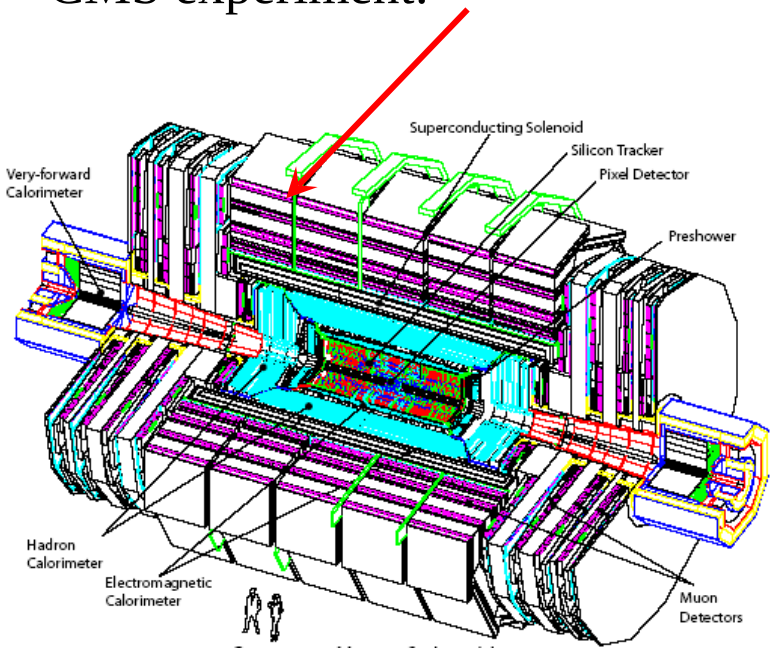

- Active surface 4000 m^2
- Gas Volume 16 m^3
- Expected rate ~ 10 Hz/cm^2

- 94.7% $C_2H_2F_4$; 5% iC_4H_{10}; 0.3 % SF_6
- 40% Relative humidity
- gas re-circulation systems

RPC electrodes: HPL

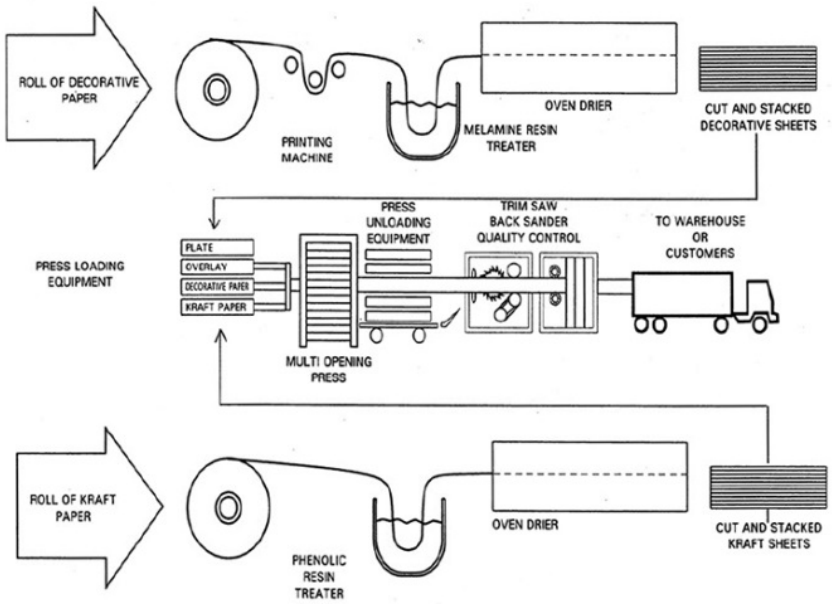

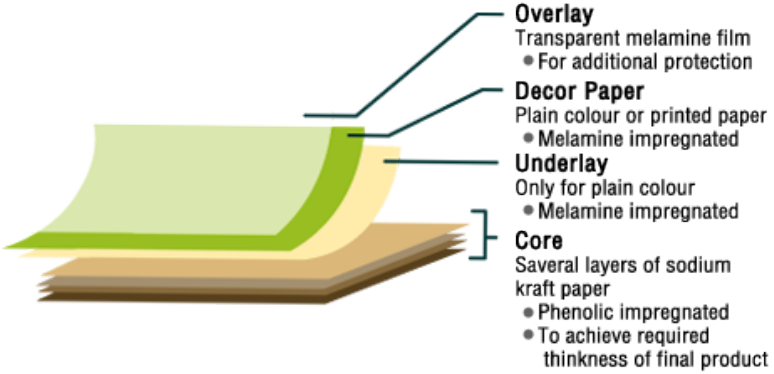

RPC: resistive electrodes

The detector rate capability is strongly dependent on the Bakelite resistivity. At high particle rate (r) the current through the detector can become high enough to produce an important voltage drop (V_d) across the electrode:

s: electrode thickness
$\langle Q_e \rangle$: average pulse charge
ρ: bakelite resistivity

In order not to lose efficiency → V_d < ~10 V

Therefore → $\rho \sim 10^{10}\ \Omega$ cm

The time constant of an elementary cell is lower at lower resistivity:

the cell is recovering faster (it is quicker ready again) after a discharge took place inside it.

RPC: resistive electrodes

It is the most important improvement with respect to previous generations

RPC equivalent circuit.

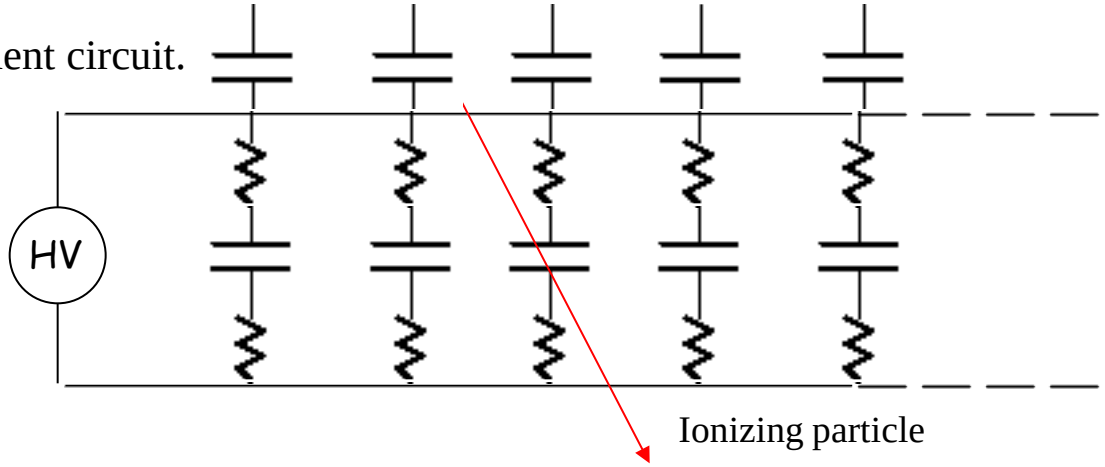

Time constant for charge development is related to drift velocity and multiplication $\tau_{discharge} = 1/\eta v_d \sim 10$ ns

Time constant for recharge the elementary cell is related to the RC $\tau_{recharge} = \rho\varepsilon \sim 10$ ms

→ $\tau_{discharge} << \tau_{recharge}$

Since $\tau_{recharge} >> \tau_{discharge}$ the arrival of the electrons on the anode is reducing the electric field and therefore the discharge will be locally extinguished.

→the electrode are like insulator after the first charge development

→Self-extinguish mechanism

RPC: resistive electrodes

What is the linseed oil:

- Drying oil (consists basically of triglycerides)
- Drying is related to C=C group in fatty acid
- Cross-linking (polymerization) in presence of air (O_2 play important role) due to C=C

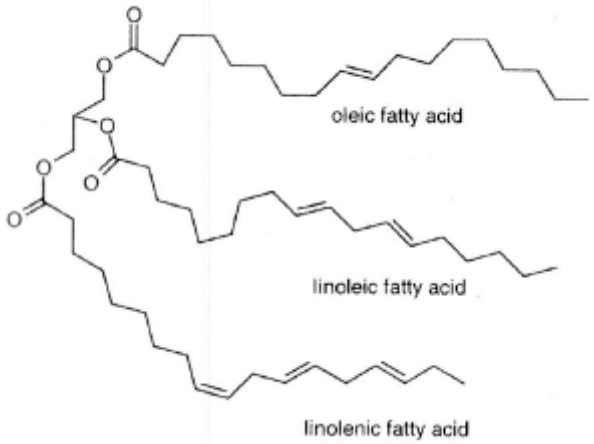

RPC electrodes are usually treated with linseed oil:

- better quality of the internal electrode surface
- it acts as a quencher for UV photons
- better detector performance

…but…

- More time needed during construction
- Ageing problems? (Not observed)

RPC: resistive electrodes

Few SEM photos (S.Ilie, C.Petitjean EST/SM-CP EDMS 344297):

Defect on Bakelite surface

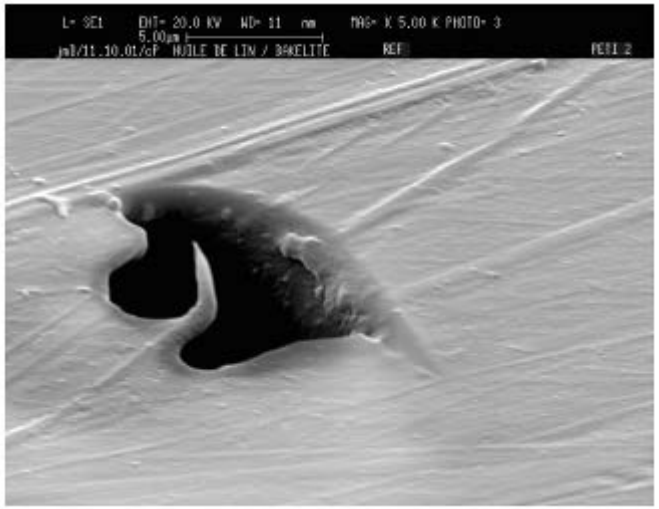

possibly covered with linseed oil

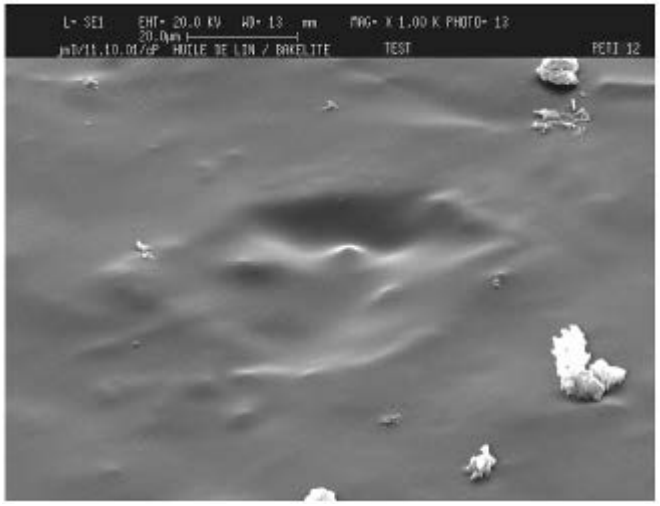

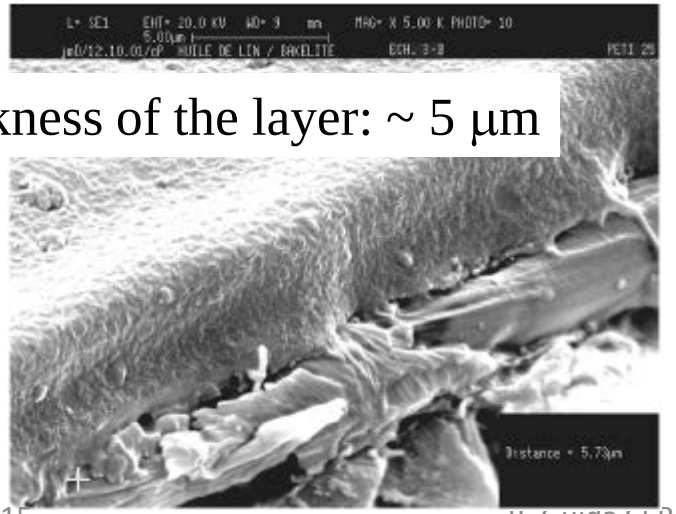

Thickness of the layer: ~ 5 µm

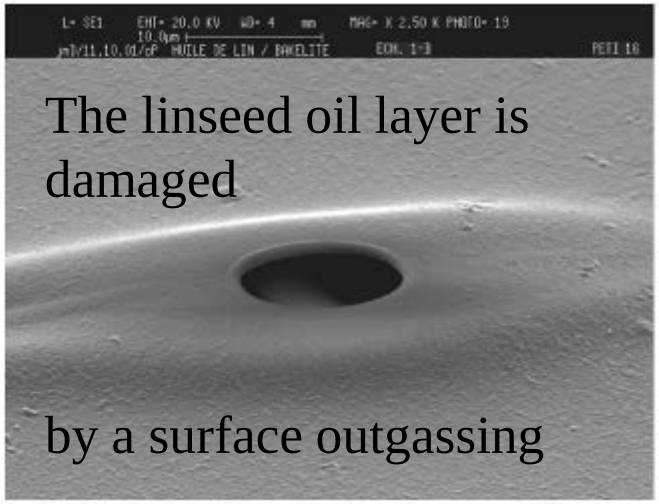

The linseed oil layer is damaged

by a surface outgassing

RPC: resistive electrodes

Effect on UV photons hitting the electrode internal surface:

Linseed oil absorbance

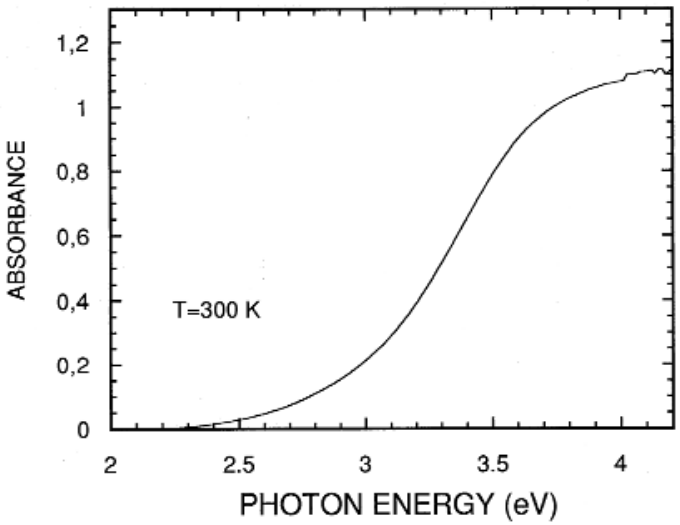

P.Vitulo NIMA 394 13-20

UV sensitivity for coated and non coated Bakelite

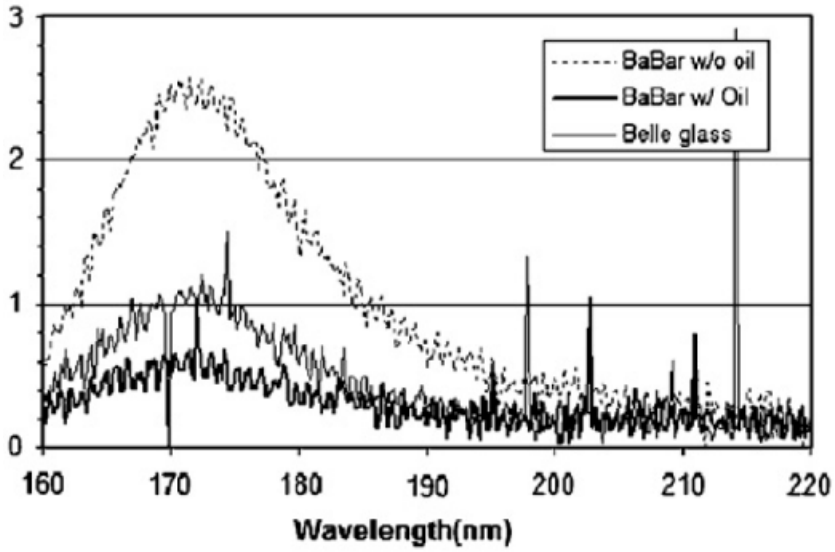

8 eV ⟷ 5.6 eV

C.Lu NIMA 602 761-765

RPC: resistive electrodes

Chamber Performance:

- With linseed oil coated electrodes
- Lower current (~1/10)
- Lower noise rate (~1/10)

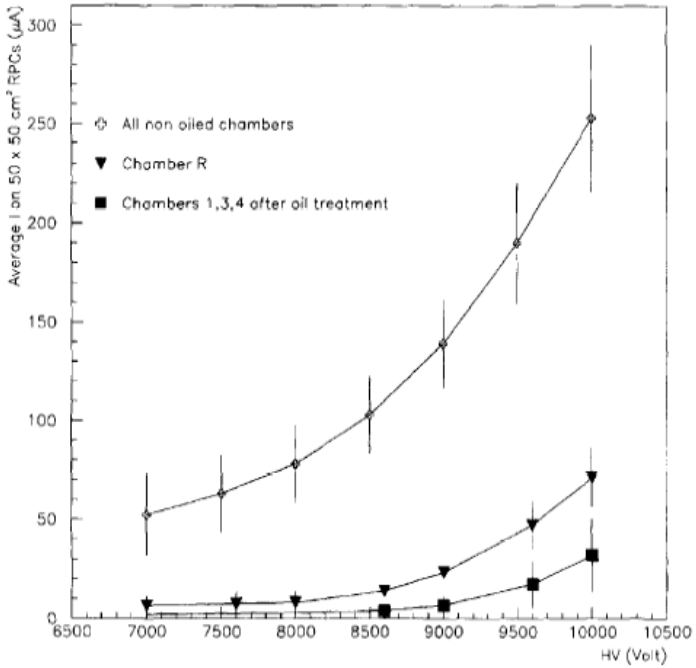

M. Abbrescia et al. NIMA 394 13-20

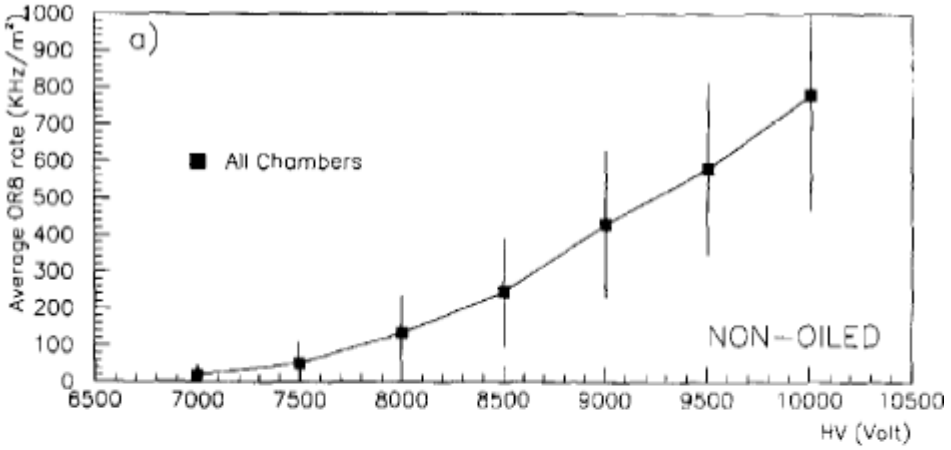

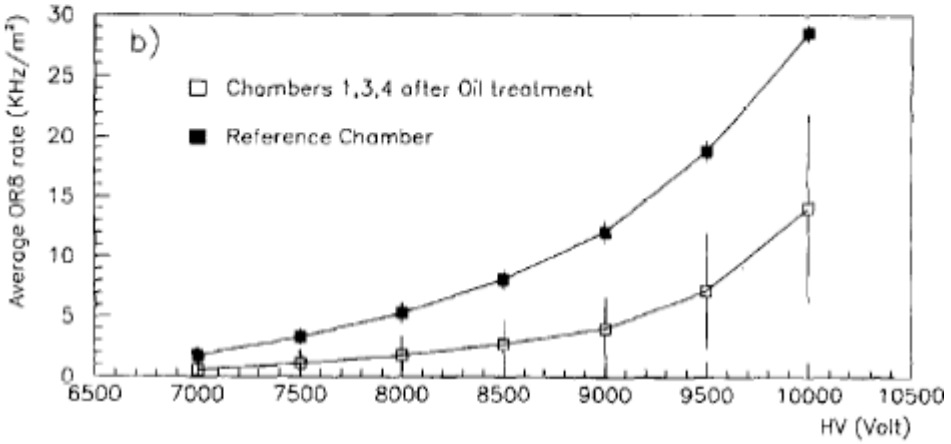

Lab session: Goals

Goals for the lab session:

- Introduction to RPC detector
- Importance of mixture composition
- Analysis of RPC signals with different gas mixtures
- Principle of gas analysis and gas systems

RPC features analyzed:

- Signal from detectors operated with different gas mixtures
- Average charge for the avalanche and streamer region.
- Average total charge.
- Event frequency for the avalanche and streamer region.

RPC signal parameters studied:

- Pulse integrated charge
- Pulse height
- Event time

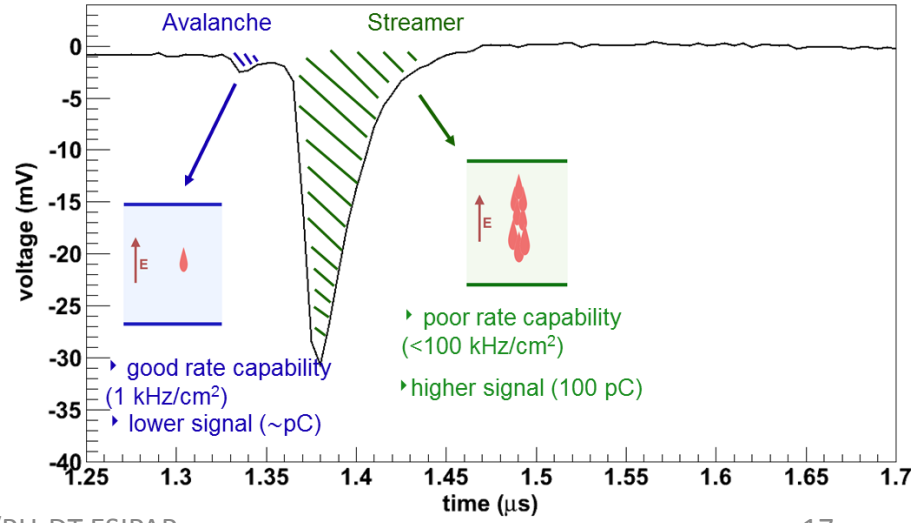

Setup description

- Standard high pressure laminate RPCs
- Scintillators (SC) for trigger on cosmic muon
- NIM modules for trigger logic and coincidences
- Data acquisition by Desktop Waveform Digitizer

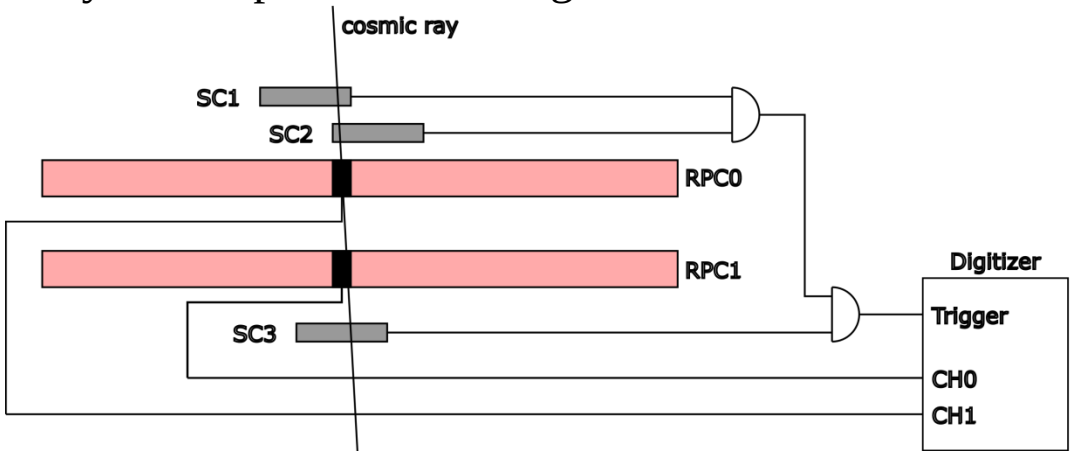

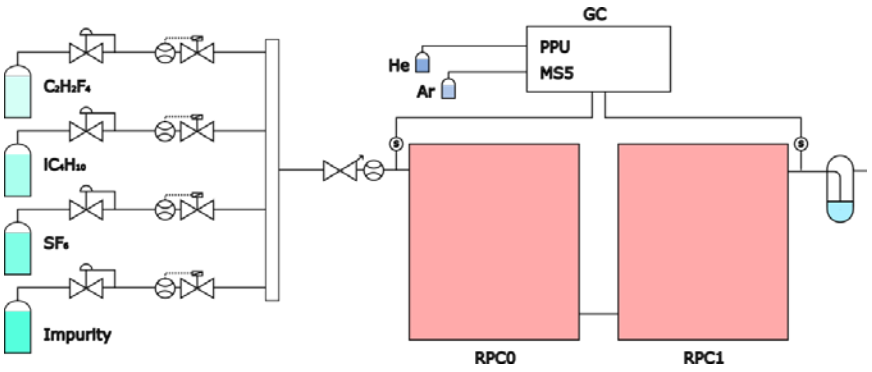

- Gas mixture composition is measured by means of a Gas Chromatograph (GC)
- Dedicated gas system for controlled injection of gas and different types of impurities

Gas systems for particle detectors

Gas systems extend from the surface building to the service balcony on the experiment following a route few hundred meters long.

- Primary gas supply point is located in surface building
- Gas system distributed in three levels:
  - Surface (SG)
  - Gas Service room (USC)
  - experimental cavern (UXC)

Large detector volume (from m^3 to several 100 m^3) and use of expensive gas components:
→
The majority is operated in closed loop gas circulation with a recirculation fraction higher than 90-95 %.

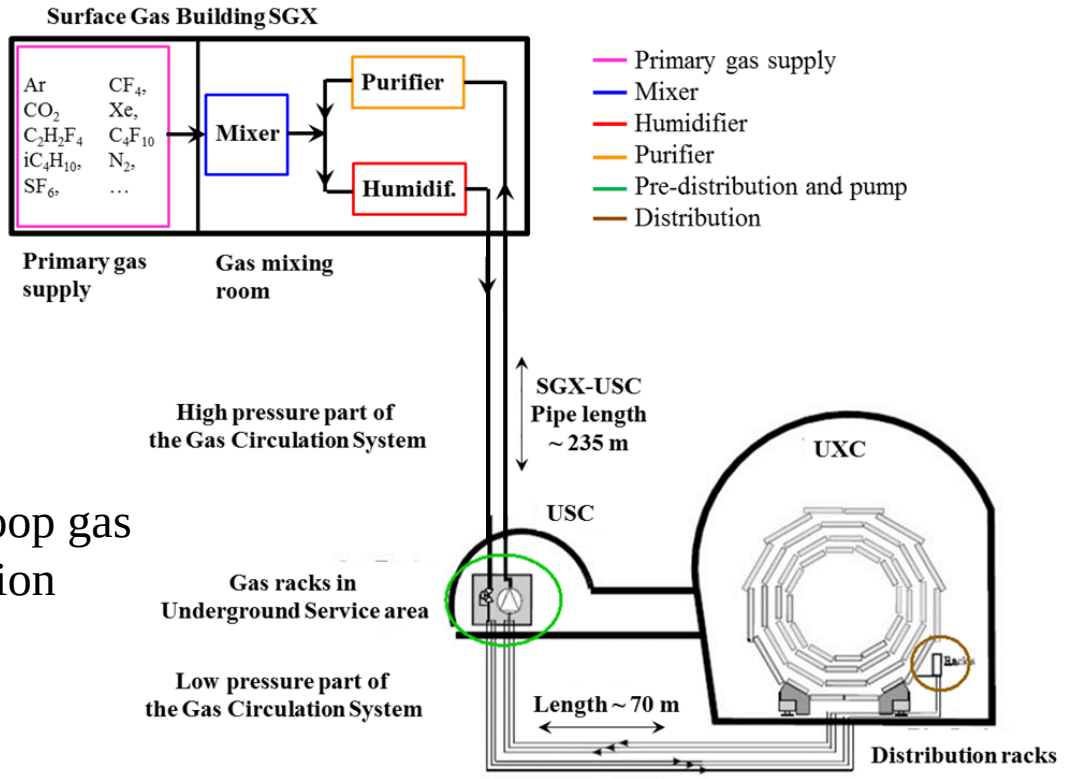

Study of different mixtures

- Setup the gas mixer for the following gas mixtures:

- Argon only
- Argon/CO_2 (70%-30%) or Argon/iC_4H_{10} (95%-5%)
- Argon/CO_2/SF_6 (69.5%-30%-0.5%) or Argon/iC_4H_{10}/SF_6 (94.5%-5%-0.5%)
- R134a/CO_2/SF_6 (69.5%-30%-0.5%) or R134a/iC_4H_{10}/SF_6 (94.5%-5%-0.5%)

- Use of gas chromatography techniques to measure the gas mixture composition

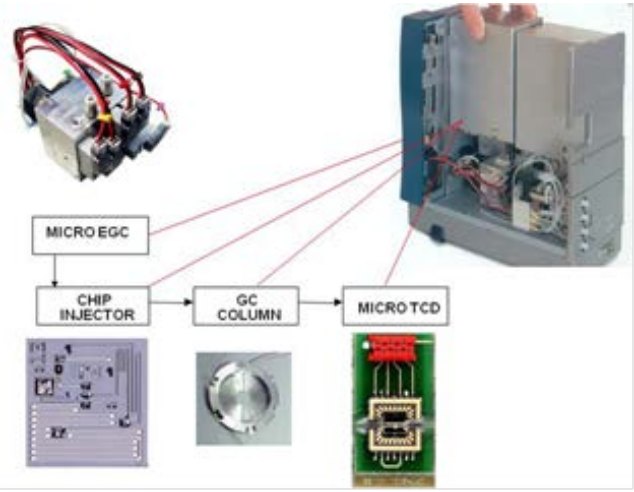

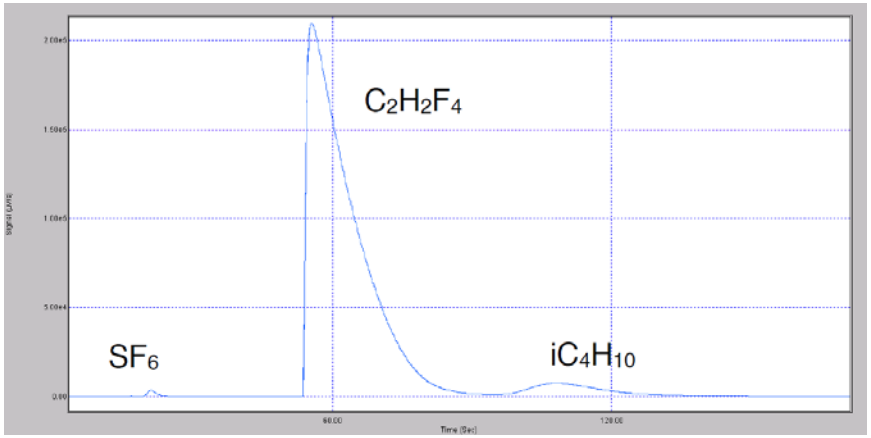

- Measurement of the pulse charge at stable mixture composition

RPC: resistive electrodes

Originally RPC were operated in *Streamer mode*:

- Ar-based mixture
- Higher signal (100 pC) but also high current in the detector
- Voltage drop at high particle rate → loss of efficiency → **poor rate capability (< 100 Hz/cm^2)**

Operation with high particle rate possible in *Avalanche mode*:

- Freon-based mixture
- lower signal (~ pC) but also lower current in the detector
- Less important high voltage drop at high particle rate → **good rate capability (~ 1 kHz/cm^2)**

Avalanche signal

Streamer signal

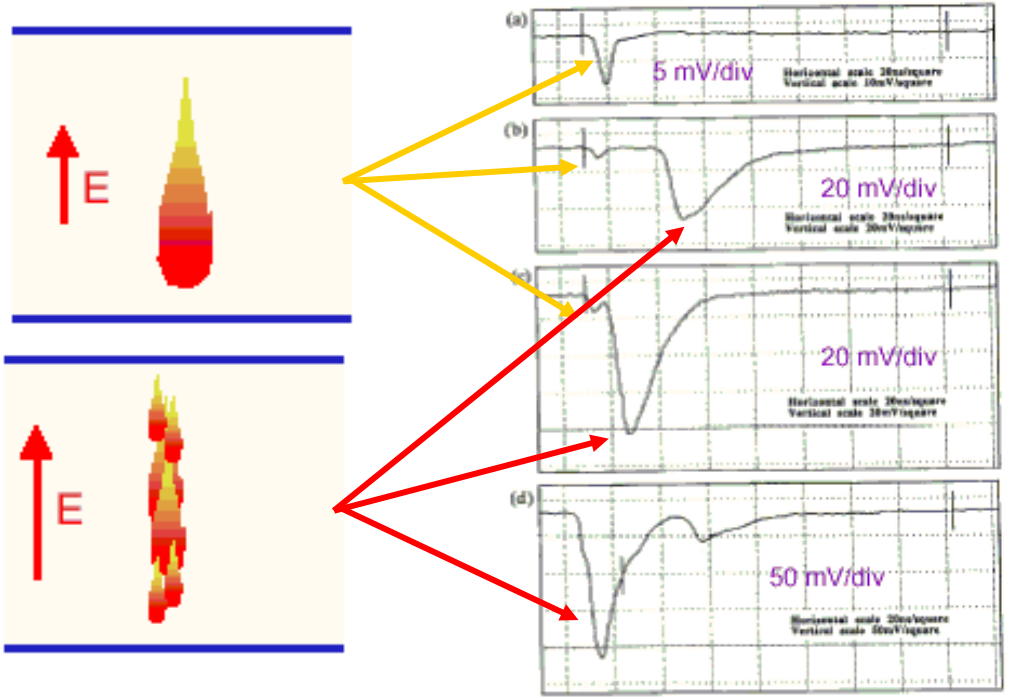

R. Santonico et al.
ATLAS Muon TDR

Measurement

Discovering the setup

- HV, DAQ and detectors (scintillators and RPCs) will be available.
- Trigger logic and DAQ will be setup during the lab session
- Looking at RPC signals with an oscilloscope

The effect of different SF_6 will be studied in detail

- Acquisition of pulse charge spectrum
- Frequency of the avalanche and streamer signals at given RPC efficiency.
- With less SF_6 the number of streamer signals is higher (at the same efficiency).
- With the increasing of the high voltage the streamer signals become predominant.

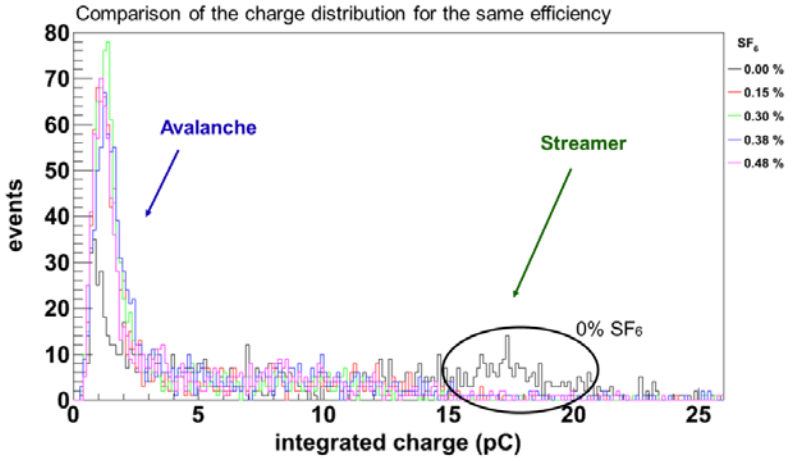

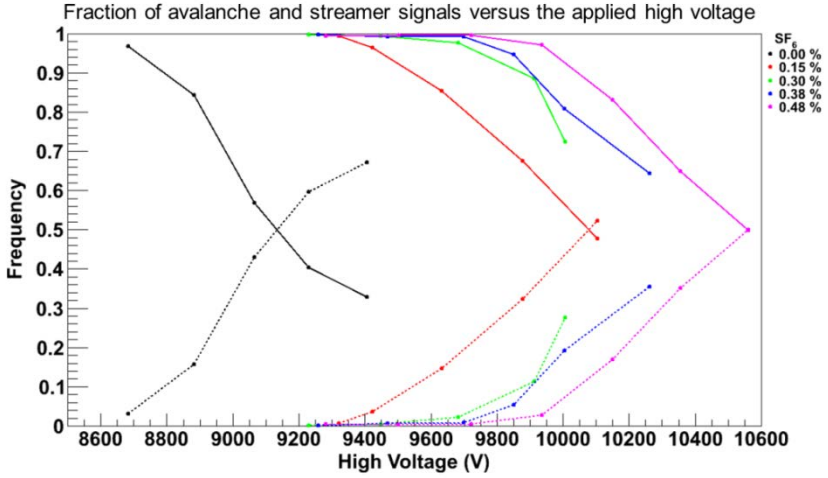

Learning goals

- Detector for triggering: RPC example
- Characteristic RPC:
  - impact of detector geometry
  - Resistive electrode
  - Signals
  - Signals vs different gas mixtures
  - Time resolution
  - Efficiency vs high voltage
  - Rate capability

- Principles of gas analysis and gas systems
- Impact of gas mixture quality and/or composition on RPC detector performances
- Extend consideration to gas detector in general

References

- R. Santonico, “Development of resistive plate counters”, Nucl.Instr. and Meth. A 187 (1981) 377-380.
- R. Guida, “The Resistive Plate Chamber detectors at the Large Hadron Collider experiments”, PH-DT Detector Seminar (https://indico.cern.ch/conferenceDisplay.py?confId=68937)
- R. Guida et al., “Optimization of a closed-loop gas system for the operation of Resistive Plate Chambers at the Large Hadron Collider experiments”, Nucl.Instr. and Meth. A 661 (2012) 214-221.
- B. Mandelli et al., “Systematic study of RPC performances in polluted or varying gas mixtures compositions: an online monitor system for the RPC gas mixture at LHC”, CERN PH- EP-Tech-Note-2012-002.

European School of Instrumentation for Particle & Astroparticle Physics (ESIPAP), lab sessions at CERN, February 5th and 12th, 2015

Laboratory Experiment: Characterization of Silicon Photomultipliers

Tutors

Dominik Dannheim, Magdalena Münker (CERN, Geneva, Switzerland)

Place

CERN, building 21, room 1-067. Telephone: +41-22-76-78195.

Abstract

This laboratory session provides an introduction to the technology of Silicon Photomultipliers (SiPM). We use a measurement setup for the characterization of single SiPM assemblies. Basic properties such as the value of the quenching resistors, the breakdown voltage, the noise rate, the cross talk and the gain are extracted.

Silicon Photomultiplier Detectors

The detectors used in this experiment are photon counters consisting of arrays of avalanche photodiodes (**APDs**) operated in Geiger mode, called Silicon Photomultiplier (**SiPM**) or Multi-Pixel Photon Counter (**MPPC**). Such devices replace conventional Photo Multiplier Tubes (PMT) for Medical Imaging applications, as for example Positron Emission Tomography (PET). They are also increasingly used in HEP applications, such as the readout of scintillators or the detection of Cherenkov light.

Figure 1 shows a photo of a SiPM. The active area is 1 mm x 1 mm and consists of 400 APDs. Figure 2 shows a schematic representation of an individual APD. A high voltage is applied to the backside of the photo diode, creating a depletion layer with high electric field in the bulk of the device. A schematic representation of the equivalent circuit of a SiPM array is shown in Figure 3 (left). Each APD is connected through an individual quenching resistor $\mathbf{R_Q}$ to a common readout. The APD array is reverse biased with a voltage above the breakdown voltage ($\mathbf{V_{BIAS} > V_B}$). In this state a single photon entering one of the APDs can, through the photo effect, create an electron-hole pair that is accelerated in the high electric field of the avalanche layer, inducing an ionization avalanche. The resulting current through the quenching resistor reduces the voltage until it falls below the breakdown voltage and the avalanche stops. The current at the output (Figure 3 (right)) therefore consists of a fast spike (<1 ns) followed by a decay with a time constant

$$\tau = R_Q * C_D. \quad (1)$$

$\mathbf{C_d}$ is the capacitance of the avalanche volume inside the APD. The signals of all APDs are readout together, such that the detected charge is proportional to the number of primary photoelectrons. The dynamic range of this measurement is limited by saturation due to the limited number of pixels.

The photon detection efficiency **PDE** of a SiPM is proportional to the quantum efficiency **QE(λ)** for photons of a given wavelength λ to create a primary photoelectron, to the efficiency for creating an avalanche ε_{aval}, and to the geometric acceptance ε_{geom} determined by the fill factor of the SiPM array. Typical PDEs for SiPMs reach about 20% for blue light.

The **gain** of the SiPM is given as the charge created per primary photoelectron:

$$G=Q/e=(V_{BIAS}-V_{BD})*C_D/e. \quad (2)$$

Typical gain values are in the range from 10^5 to 10^6. Both gain and breakdown voltage change with temperature. An increased temperature leads to increased thermal vibrations in the silicon lattice, reducing the free path length of the accelerated charges. The breakdown voltage therefore increases with increasing temperature (few tens of mV/K), while the gain for a given overvoltage decreases (few %/K).

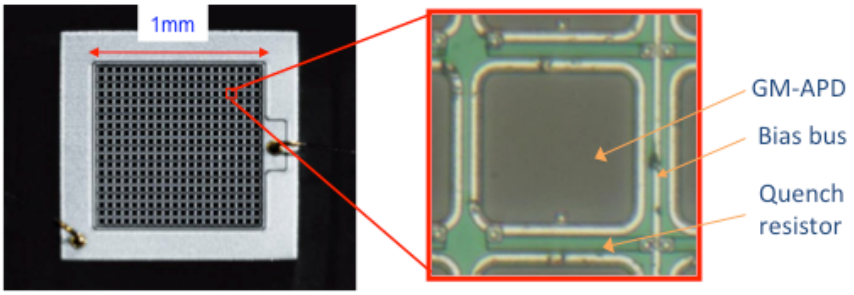

Figure 1: Photograph of a SiPM with 400 APDs

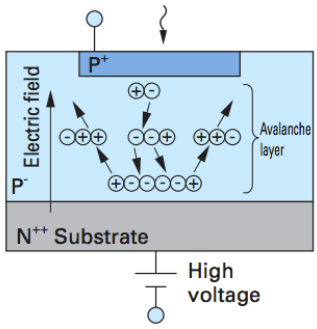

Figure 2: APD schematic

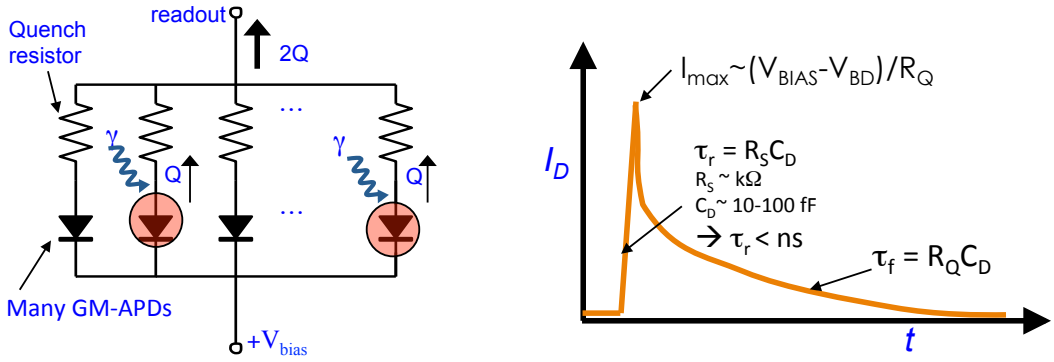

Figure 3: SiPM schematic (left) and current pulse initiated by an avalanche in an APD (right)

Besides photons or other particles traversing the APDs, also thermal/tunneling charge carrier generation can trigger an avalanche. The signal of such **noise pulses** is identical to the one created by a single photoelectron. The rate of noise pulses can reach a few MHz and increases with temperature.

Optical **cross talk** occurs when photons created in the avalanche initiate another avalanche in a neighboring cell, leading to an observed pulse corresponding to two or more photoelectrons. Cross talk occurs typically for about 10% of all pulses.

After pulses occur when ionization charges trapped in impurities of the silicon lattice get released with a delay of up to several hundreds of nanoseconds, initiating

another avalanche. Depending on the delay they either lead to distorted pulses or additional pulses. Typically a few percent of all avalanches lead to after pulses.

Measurement setup

A Hamamatsu S10943-8584 **SiPM** is used for this experiment. It consists of 400 pixels in an area of 1 mm x 1 mm. The recommended operation bias voltage at a temperature of 25 °C is 71.5 V. The temperature dependence of the breakdown voltage is approximately 55 mV/K.

Figure 4 shows a photo of the **test box** used for the experiment. An external **LED pulser** is used to create photons that are detected by the SiPM connected to an amplifier circuit.

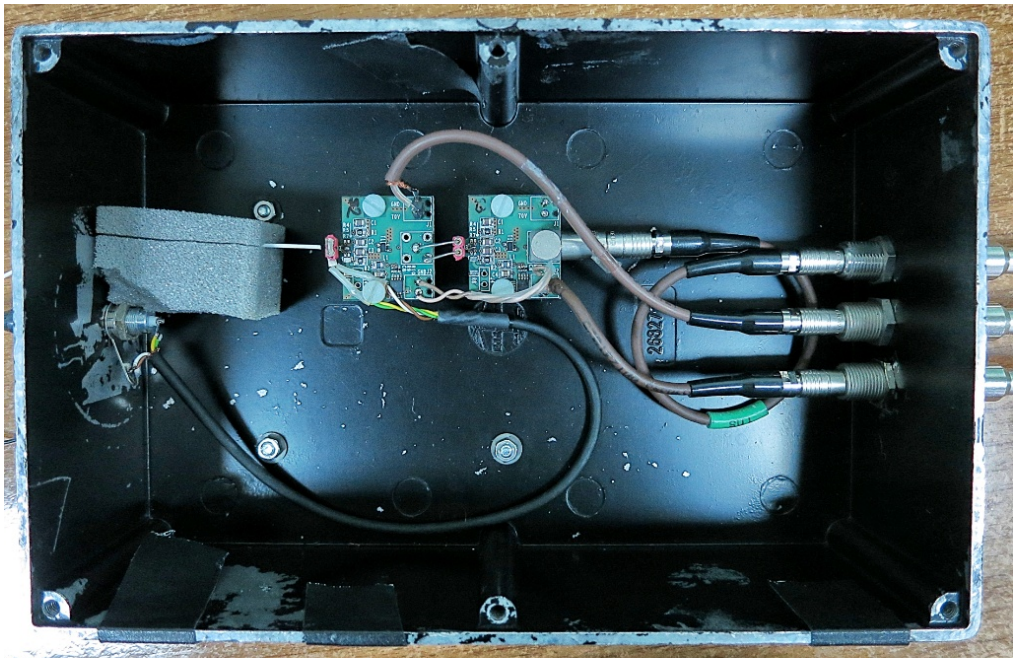

Figure 4: Measurement box with amplifier boards

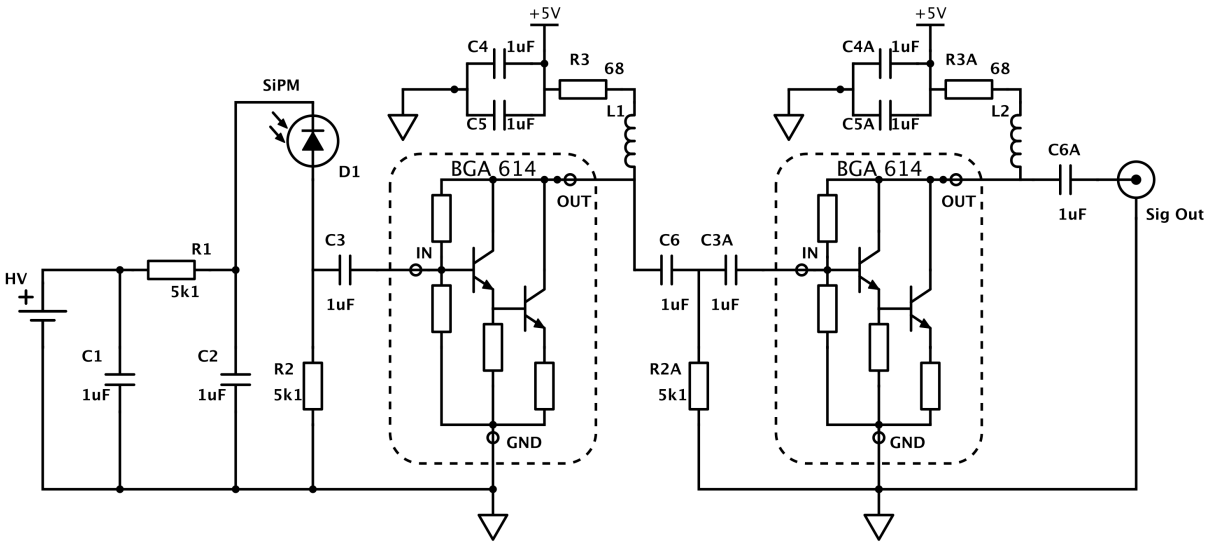

Figure 5: SiPM biasing and readout circuit

The SiPM is mounted on a PCB containing the **biasing** circuit and a one-stage **amplifier**. The amplifier converts the current signal from the SiPM to a voltage signal. It is based on a BGA614 amplifier with a fixed gain of 9. The amplifier output is connected to another amplifier of the same type on a separate PCB. Figure 5 shows the schematic of the biasing circuit and the two amplification stages. A **PT 1000** temperature sensor is used to monitor the temperature close to the SiPM.

The sensitive side of the SiPM faces an optical fiber coupled to an external **LED pulser** providing very short (~ns) light pulses of low intensity. Figure 6 shows a photo and a simplified schematics of the LED pulser. The fast switch S1 is implemented with a transistor. Its base is connected to an external trigger. The resistor R1 acts as a quenching resistor for the LED. When the switch is closed, the LED gets powered through the capacitor C1 and produces light until the voltage at the output of R1 drops below the threshold voltage of the LED (~1.5 V). The light intensity is regulated with the bias voltage V_{LED}.

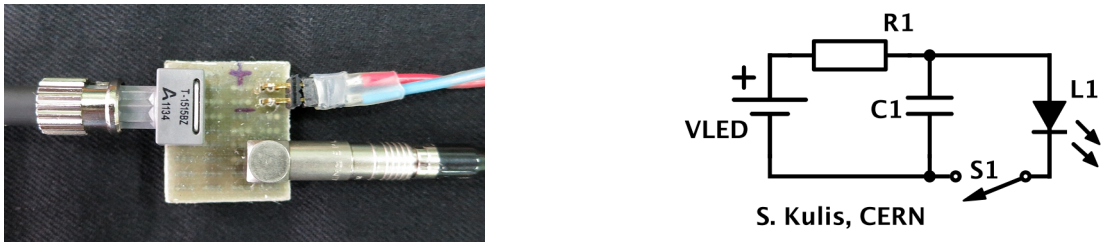

Figure 6: Photo (left) and simplified schematics (right) of the LED pulser

The output of the second amplifier stage is connected to a 500 MHz Picoscope 6404D **oscilloscope** used for the data acquisition. It also includes a **signal-generator** providing the trigger both for the LED pulser and for the oscilloscope readout. The oscilloscope is controlled by a laptop via a USB connection. The data from the oscilloscope is displayed and analyzed with a LabVIEW program.

The amplifier and the LED pulser are powered by an external Gossen 33K7 **Low-voltage power supply**. A Keithley 2410 **HV source meter** provides the high voltage for the SiPM and measures the current through the SiPM. A Fluke 45 **multimeter** is used to measure the resistance of the PT 1000 temperature probe.

Measurement 1: Value of the quenching resistors

In this exercise we determine the value of the quenching resistors through a measurement of the forward-bias current characteristic.

- Connect the HV source to the measurement box.
- Take current measurements in small steps from 0 to approximately -2 V and record them in the provided spreadsheet.
- Make a plot of the current versus voltage. Extract the resistance from a fit to the linear part of the curve.
- The amplifier board contains additional series resistors. Find them in the schematic (Figure 5). *[Optional: Confirm their values with a resistance measurement, after removing the SiPM.]* Calculate the average value of the quenching resistors, Rq, taking into account the series resistors on the amplifier board and the total number of APDs.

Measurement 2: Noise rate and cross talk

In this exercise we measure the noise rate of the device and determine the fraction of pulses with cross talk.

- Connect the low-voltage and high-voltage inputs of the box to the respective devices. Connect the signal output to input A of the oscilloscope.
- Measure the temperature at the SiPM through the PT 1000 resistance. Wait until it stabilizes. Note the temperature in the provided spreadsheet.
- Use the Picoscope software to control the oscilloscope. Turn on channel A (+-100 mV, 50 Ohm). Trigger on channel A, falling edge, and set the trigger level to be within the noise.
- Set the high voltage initially to 68 V and increase it in steps of 1 V, until the signal from thermal noise appears on the oscilloscope screen. Now set the high voltage to the recommended operating voltage, taking into account the temperature dependence of the breakdown voltage:
  V_{BIAS} = 71.5 V + (T [°C] - 25 °C) * 0.055 V.
  Set the trigger to rising edge and a level of approximately 20 mV, which should be somewhat outside the noise fluctuations.
- Set the time window of the acquisition to 10 ms.
- A peak detection algorithm is used to count the number of noise peaks in the acquisition window. The number of peaks above the thresholds for >=1 photoelectron pulses and >=2 photo-electron pulses are displayed in the box below the oscilloscope. Check and if necessary adjust the two trigger thresholds for >=1 photoelectron pulses and >=2 photo-electron pulses. Adjust the acquisition window if necessary.
- Note the values for >=1 and >=2 photoelectron pulses in the spreadsheet.
- [Optional: Repeat the measurement for decreased and increased bias voltages (-0.5 V, +0.5 V, +1.0 V). Check the temperature before each measurement. Adjust the trigger thresholds depending on the observed signal levels. Plot the noise rate as function of operation voltage.]

Measurement 3: Gain, capacitance and breakdown voltage

In this exercise we use the LED pulser to create photons entering the SiPM. We determine the gain, capacitance and breakdown voltage of the device by an analysis of the pulse integrals for different operation voltages. Finally we estimate the signal fall time and the depth of the avalanche region inside the APDs.

- Use the same connections and operation voltage setting as for the previous measurement. In addition, connect the signal-generator output of the oscilloscope to input channel B of the oscilloscope and extend this signal to the trigger input of the box.
- Use 100 kHz square pulses, with a level setting from -2 to 2 V. Turn on channel B (±1 V, 1 MOhm).
- Trigger on channel B at a level of 0 V, falling edge. Set the post-trigger time window to 100 ns and the pre-trigger time window to 50 ns. Adjust the LED pulse intensity by changing the bias voltage of the LED pulser, until you observe the pulses from the LED light.
- Measure the SiPM temperature using the PT 1000 and note the value in the provided spreadsheet.

- The histogram window shows several peaks, corresponding to pulses with 0, 1, 2, … photo electrons. Adjust the LED pulse intensity until you see the maximum of the histogram at 1 or 2 photoelectrons. Perform a Gaussian fit of the peaks for 1 and 2 photo electrons. Adjust the fit range using the cursors to cover the respective peaks. Note the obtained mean values in the spreadsheet.
- Calculate the average charge Q for a single photo-electron pulse based on the difference between the two peaks, taking into account the amplifier gain of 81 and the 50 Ohm measurement resistor of the oscilloscope. Calculate the SiPM gain G using equation 2. *[Optional: fit also the 4^{th} and 5^{th} peak of the histogram and use the average of the differences between the mean values to calculate the charge and SiPM gain.]*
- Repeat the measurement and analysis three more times for different bias voltages below and above the nominal one: -0.5 V, +0.5 V, +1.0 V. Plot gain versus operation voltage and obtain the breakdown voltage V_{BD} from a linear fit.
- Calculate the capacitance C_D (equation 2) and use it together with R_Q to determine the expected fall time of the signal (equation 1). Compare it to the fall time observed on the oscilloscope.
- Calculate the depth d of the avalanche volume, assuming that the capacitance of the APD is given by its geometry:
  $C_D=\varepsilon_{Si}*\varepsilon_0*A/d$,
  with $\varepsilon_{Si}=11.7$, $\varepsilon_0=8.854*10^{-12}$ F/m. The area A of a single APD can be estimated from Figure 1.